



# Relationships between Quality and Attributes of Spot Welds

*A spot weld's strength can be determined by the geometric characteristics and mechanical properties of the weldment*

BY M. ZHOU, H. ZHANG, AND S. J. HU

**ABSTRACT.** A resistance spot weld's strength is determined by the physical attributes of the weldment. However, it is extremely difficult to establish a universal relationship with experiments between the measurable attributes of a weld and the weld's quality. The large number of variables and experimental uncertainty inhibit establishing such a relation. A computer simulation experiment was conducted in this study, using the concept of design of experiments, to overcome the shortcomings of traditional experimental investigations. Quantitative relationships were established to link a weld's geometric and mechanical attributes to its strength under tensile-shear loading.

## Introduction

Spot weld quality is a loosely defined term, and it is usually measured against the performance requirements of a weld. They can be either quantitative or qualitative. In general, weld performance characteristics should refer to both static and dynamic strength. Tensile-shear strength, cross-tension strength, and peel strength are examples of static strengths, and impact and fatigue strengths are commonly referred to as the dynamic strengths. However, because of practical reasons, only tensile-shear tests are conducted in most cases. Typically, the strength of a spot-welded joint is often related to the joint's physical attributes. In addition to weld button size (usually obtained after a peel test), as shown in Fig. 1, a weld's at-

tributes usually refer to nugget/button size, size of heat-affected zone (HAZ), penetration, indentation, sheet separation, and material properties (Ref. 1). However, only button size has been used extensively in attribute-strength relationships. Other weld attributes are rarely used, primarily because it is not clear how they affect the quality or strength of spot welds.

Spinella (Ref. 2) suggested that good welds are welds with large buttons and high tensile strength without expulsion or a partial button. In Newton et al. (Ref. 3), a weld with a full-size nugget and at least minimum strength, and without cracks, flash (expulsion), or porosity, was regarded as a good weld. Their study also tried to define nonconformable welds as those of too small weld size, or with cracks, excessive porosity, excessive expulsion, and damaged adhesive layers for weld-bonding. These classifications are generally qualitative and depend on multiple parameters, in addition to the materials welded (steel or aluminum). In many cases, the nugget width or button diameter is used as the sole parameter to describe the quality of a spot weld. This is because, intuitively, the joint size should have the biggest influence on weld

strength. It is also easy to measure, and specific values of weld button size are often given in standards and requirements. There are many attempts to link weld size to weld quality/strength. The majority of such work is on the relationship between weld diameter and tensile-shear strength.

An early work in this aspect is a simple expression of strength as a function of weld diameter developed by Keller and Smith (Ref. 4) and by McMaster and Lindrall (Ref. 5)

$$P = 120d^2 \quad (1)$$

where  $P$  is shear load in newtons and  $d$  is weld diameter in mm.

Heuschkel (Ref. 6) proposed a more complex empirical relationship for tensile-shear strength

$$S = t \cdot S_0 \cdot d \cdot [\alpha - \beta(C + 0.05Mn)] \quad (2)$$

where  $S$  is tensile-shear strength,  $S_0$  is base metal (BM) strength,  $d$  is weld diameter,  $t$  is sheet thickness,  $C$  and  $Mn$  are compositions of BM chemistry, and  $\alpha$  and  $\beta$  are functions of thickness  $t$ . It depends on both joint dimensions and material properties. However, such a complex relationship is not preferred for strength prediction. Following Heuschkel's work, Sawhill and Baker (Ref. 7) proposed a similar formula for rephosphorized and stress-relieved steels,

$$S = f \cdot t \cdot S_0 \cdot d \quad (3)$$

where  $f$  is a material-dependent coefficient,  $f = 2.5 \sim 3.1$ . Although the majority of work has been done on steels, some efforts have been devoted to aluminum welding as aluminum alloys have been introduced in automotive assembly in the

## KEY WORDS

Dynamic Strength  
 Finite Element Method  
 Resistance Welding  
 Spot Welding  
 Static Strength  
 Weld Nugget

M. ZHOU and S. J. HU are with Department of Mechanical Engineering, University of Michigan, Ann Arbor, Mich. H. ZHANG is with Department of Mechanical, Industrial, and Manufacturing Engineering, University of Toledo, Toledo, Ohio.

last decade or so. By considering the fracture mode, an expression was proposed for aluminum alloys by Thornton et al. (Ref. 8)

$$P = (0.12t - a)d \quad (4)$$

Here  $P$  is in kN,  $t$  and  $d$  are in mm, and  $a$  is the coefficient of fracture mode.

These equations provide valuable information on the dependence of weld strength on weld dimensions. However, they are suitable only for specific materials and weld joint geometries. Ewing et al. (Ref. 9) tried to develop a relationship between spot weld failure load and BM strength, testing speed, joint configuration, and welding schedule. Several tests, such as tensile-shear, cross-tension, and coach-peel, were conducted on various automotive body materials to establish the relationship. The results were scattered mainly due to the complexity of the fracture process of spot-welded joints and the large number of variables involved in the experiment.

Since shear strength and weld size are closely related, requirements are commonly made on weld size, which in turn, is often designed based on the thickness of the sheets. An optimum weld diameter was considered to be  $5\sqrt{t}$ , where  $t$  is sheet thickness in mm (Ref. 10). In U.S. Standard units (inches), this optimum diameter is approximately  $\sqrt{t}$ . Current industrial applications set weld diameter between  $3\sqrt{t}$  and  $6\sqrt{t}$  mm. Such requirements assume a clear dependence of weld strength on weld size. However, as pointed out by Dickinson (Ref. 11), a correlation between strength and weld diameter does not always exist. Except for weld size, there is very little research about the influence of weld attributes, such as heat-affected zone (HAZ), indentation, etc., on spot weld quality. The importance of material properties has been long recognized; however, only recently have people started to distinguish the effects of material properties in different parts of a weldment such as the nugget, HAZ, and base metal (Refs. 12, 13).

In this paper, a detailed computer model of spot-welded joints is presented and a computer design of experiments is introduced to evaluate the spot weld strength. The effects of weld attributes on weld quality/strength, and the relationship between weld strength and weld attributes have been quantitatively established.

## Weld Attributes and Weld Strength

The finite element method (FEM) has become a powerful tool for numerical solutions to a wide range of engineering

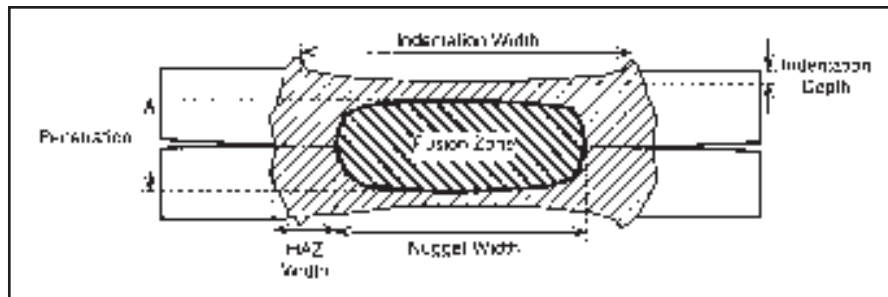


Fig. 1 — A weld's geometric attributes, as shown in a schematic cross section of a spot weldment (Ref. 1).

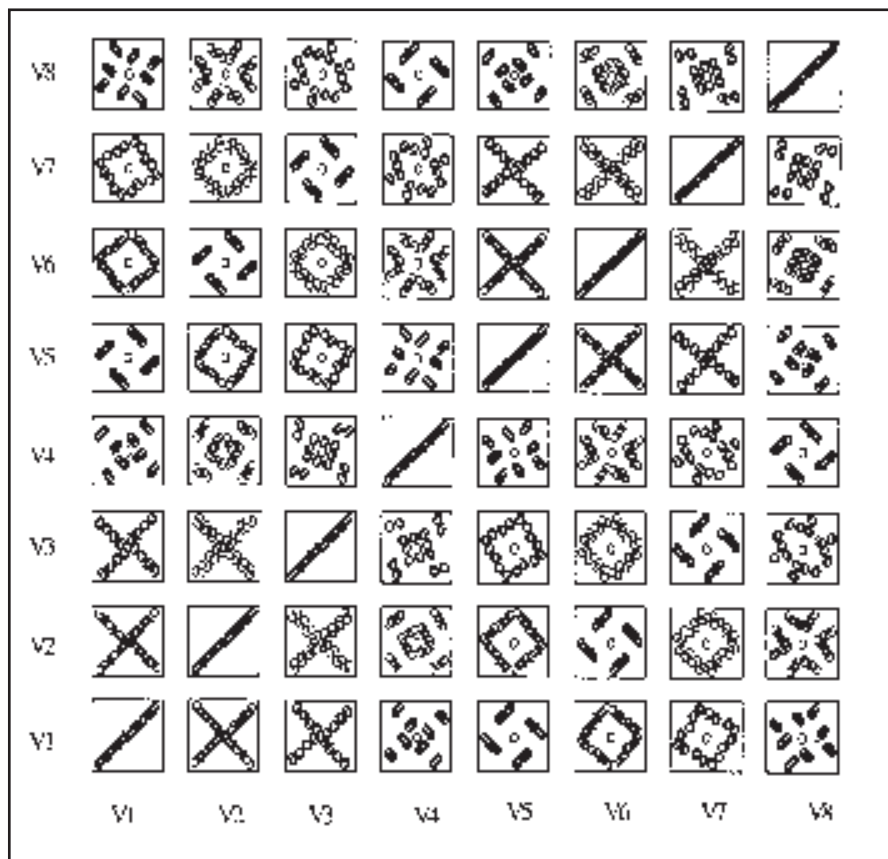


Fig. 2 — Distribution of the Latin hypercube design.

Table 1 — Ranges of Input Variables

t (mm)	h (mm)	w (mm)	$t_f$	$\sigma_f$ (MPa)	$\sigma_0$ (MPa)	e (%)	k
0.5 ~ 2.0	0.1 ~ 1.5	30 ~ 50	0 ~ 20%	205 ~ 1725	50 ~ 200	2 ~ 65	1.0 ~ 3.0

problems. With the aid of statistical design and the advances in computer technology and computer-aided design (CAD) systems, FEM can provide a quick and accurate solution for a very complex problem with relative ease. Using this numerical procedure, the uncertainties associated

with experiments can be avoided and the cost can be significantly reduced. Therefore, FEM is employed to analyze the quality of a spot-welded joint.

Based on previous studies (Ref. 14), a weld's strength can be fully expressed by its peak load and corresponding energy

**Table 2 — Matrix of Latin Hypercube Design (in coded scale)**

var1	var2	var3	var4	var5	var6	var7	var8
1	-2	-4	-8	-16	15	13	-9
2	1	-3	-7	-15	-16	14	-10
3	-4	2	-6	-14	13	-15	-11
4	3	1	-5	-13	-14	-16	-12
5	-6	-8	4	-12	11	9	13
6	5	-7	3	-11	-12	10	14
7	-8	6	2	-10	9	-11	15
8	7	5	1	-9	-10	-12	16
9	-10	-12	-16	8	-7	-5	1
10	9	-11	-15	7	8	-6	2
11	-12	10	-14	6	-5	7	3
12	11	9	-13	5	6	8	4
13	-14	-16	12	4	-3	-1	-5
14	13	-15	11	3	4	-2	-6
15	-16	14	10	2	-1	3	-7
16	15	13	9	1	2	4	-8
0	0	0	0	0	0	0	0
-16	-15	-13	-9	-1	-2	-4	8
-15	16	-14	-10	-2	1	-3	7
-14	-13	15	-11	-3	-4	2	6
-13	14	16	-12	-4	3	1	5
-12	-11	-9	13	-5	-6	-8	-4
-11	12	-10	14	-6	5	-7	-3
-10	-9	11	15	-7	-8	6	-2
-9	10	12	16	-8	7	5	-1
-8	-7	-5	-1	9	10	12	-16
-7	8	-6	-2	10	-9	11	-15
-6	-5	7	-3	11	12	-10	-14
-5	6	8	-4	12	-11	-9	-13
-4	-3	-1	5	13	14	16	12
-3	4	-2	6	14	-13	15	11
-2	-1	3	7	15	16	-14	10
-1	2	4	8	16	-15	-13	9

and displacement at peak load under tensile-shear testing. Intuitively, they can be expressed as functions of the joint geometry and material properties, or

$$P_{max} = f_P(\text{geometry; material properties of base metal, HAZ, and nugget}) \quad (5A)$$

$$U_{max} = f_U(\text{geometry; material properties of base metal, HAZ, and nugget}) \quad (5B)$$

$$W_{max} = f_W(\text{geometry; material properties of base metal, HAZ, and nugget}) \quad (5C)$$

where  $P_{max}$  is the peak load, and  $U_{max}$  and  $W_{max}$  are corresponding displacement and energy, respectively. In general, all these relationships are unknown. It is also very difficult, if not impossible, to derive them analytically. Different approaches must be sought in order to develop such relations. Therefore, a newly developed methodology with combined numerical approach (FEM) and statistical planning and analysis (design of experiments) (Ref. 15) is employed to establish such relationships.

### Design of Numerical Experiments

The use of design of experiments in numerical experiments has several distinctive differences from conventional designs of experiments of physical tests, as dis-

**Table 3 — Matrix of Latin Hypercube Design (in natural scale)**

Run	t	h	w	t <sub>i</sub>	σ <sub>y</sub>	σ <sub>un</sub> -σ <sub>y</sub>	u	k	U <sub>max</sub>	P <sub>max</sub>	W <sub>max</sub>	J <sub>c</sub>
1	1.27	0.74	37.88	0.055	251.06	190.91	0.58	1.48	1.30	4.53	4683	4.48E-07
2	1.32	0.82	38.48	0.061	297.12	54.55	0.60	1.42	0.93	3.86	2960	5.16E-07
3	1.36	0.65	40.91	0.067	343.18	181.82	0.10	1.36	1.06	5.32	4528	4.78E-07
4	1.41	0.91	40.30	0.073	389.24	63.64	0.08	1.30	0.78	4.92	3003	4.51E-07
5	1.45	0.57	35.45	0.121	435.30	172.73	0.51	2.76	1.38	8.45	8845	4.57E-07
6	1.50	0.99	36.06	0.115	481.36	72.73	0.52	2.82	1.03	8.43	6359	4.26E-07
7	1.55	0.48	43.33	0.109	527.42	163.64	0.17	2.88	0.58	8.82	3120	3.72E-07
8	1.59	1.08	42.73	0.103	573.48	81.82	0.15	2.94	1.00	11.02	7735	3.54E-07
9	1.64	0.40	33.03	0.006	1310.45	95.45	0.27	2.03	0.86	15.51	68	3.67E-07
10	1.68	1.16	33.64	0.012	1264.39	159.09	0.26	2.09	1.79	22.78	26730	3.40E-07
11	1.73	0.31	45.76	0.018	1218.33	104.55	0.47	2.15	0.44	11.03	2448	2.75E-07
12	1.77	1.25	45.15	0.024	1172.27	150.00	0.49	2.21	1.63	24.10	26740	2.77E-07
13	1.82	0.23	30.61	0.170	1126.21	113.64	0.35	1.73	0.53	10.30	2710	3.34E-07
14	1.86	1.33	31.21	0.164	1080.15	140.91	0.33	1.67	1.44	19.59	18260	3.12E-07
15	1.91	0.14	48.18	0.158	1034.09	122.73	0.40	1.61	0.18	4.72	416	2.22E-07
16	1.95	1.42	47.58	0.152	988.03	131.82	0.42	1.55	1.42	20.07	20540	2.37E-07
17	1.25	0.80	40.00	0.100	965.00	125.00	0.36	2.00	1.05	11.25	7609	5.58E-07
18	0.55	0.18	32.42	0.048	941.97	118.18	0.29	2.45	0.87	3.46	1988	2.63E-06
19	0.59	1.46	31.82	0.042	895.91	127.27	0.31	2.39	0.81	3.94	1976	2.24E-06
20	0.64	0.27	48.79	0.036	849.85	109.09	0.38	2.33	0.80	4.09	2260	1.81E-06
21	0.68	1.37	49.39	0.030	803.79	136.36	0.36	2.27	0.76	4.52	2321	1.57E-06
22	0.73	0.35	34.85	0.176	757.73	100.00	0.22	1.79	0.62	3.78	1476	1.60E-06
23	0.77	1.29	34.24	0.182	711.67	145.45	0.24	1.85	0.72	4.05	1938	1.41E-06
24	0.82	0.44	46.36	0.188	665.61	90.91	0.45	1.91	0.56	4.08	1512	1.20E-06
25	0.86	1.20	46.97	0.194	619.55	154.55	0.44	1.97	0.68	4.47	2141	1.07E-06
26	0.91	0.52	37.27	0.097	1356.52	168.18	0.56	1.06	1.08	8.22	5698	1.01E-06
27	0.95	1.12	36.67	0.091	1402.58	86.36	0.54	1.12	1.12	8.61	6306	9.23E-07
28	1.00	0.61	43.94	0.085	1448.64	177.27	0.19	1.18	1.07	10.21	6978	8.05E-07
29	1.05	1.03	44.55	0.079	1494.70	77.27	0.20	1.24	1.09	10.57	7518	7.34E-07
30	1.09	0.69	39.70	0.127	1540.76	186.36	0.63	2.70	1.41	14.96	13010	7.18E-07
31	1.14	0.95	39.09	0.133	1586.82	68.18	0.61	2.64	1.34	14.92	12360	6.69E-07
32	1.18	0.78	41.52	0.139	1632.88	195.45	0.11	2.58	1.39	16.67	14390	6.13E-07
33	1.23	0.86	42.12	0.145	1678.94	59.09	0.13	2.52	1.25	16.72	12580	5.60E-07

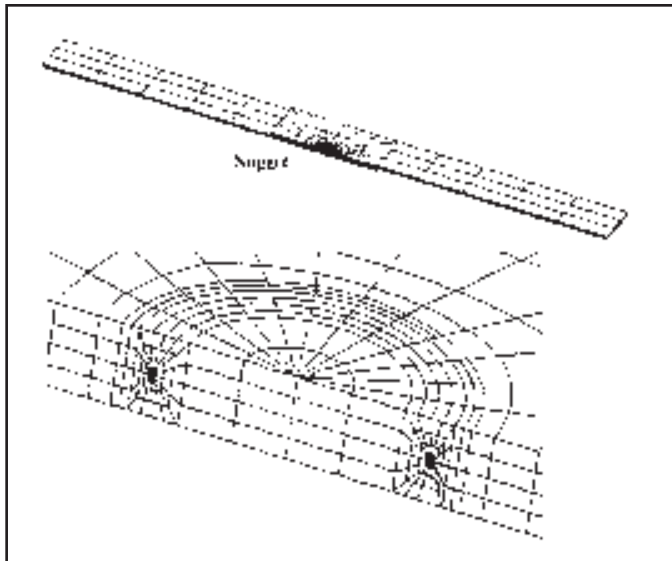


Fig. 3 — A generic finite element model.

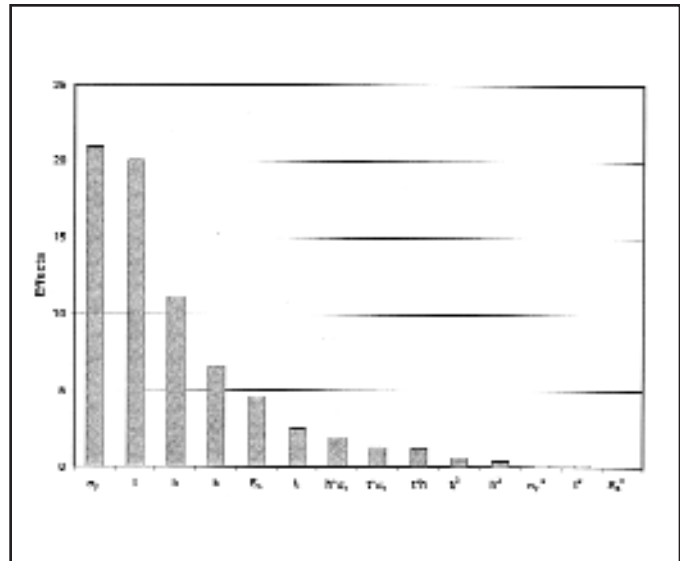


Fig. 4 — Variable effects on maximum load  $P_{max}$ .

cussed in Zhou et al. (Ref. 14). For instance, significantly more information can be obtained using fewer number of runs compared to conventional design of experiments. Procedures for the design are detailed in the following sections for quality evaluation of spot-welded specimens.

### Selection of Variables

As in conventional design of experiments, the first task is to choose experiment variables. There are two sets of variables needed in this study. One is for geometric dimensions, which include sheet thickness, specimen length, specimen width, sheet overlap, nugget diameter, HAZ size, indentation, sheet separation, and so on. Based on previous studies (Ref. 14), the length is fixed at  $L = 150$  mm, and the overlap is equated to the width of the specimen. For simplicity, only large-size welds are taken into account, and the nugget diameter is linked to the sheet thickness by  $d = 5\sqrt{t}$ . The extreme case for a welded joint, where there is a sharp notch around the nugget, was considered. Therefore, geometrical variables were chosen as sheet thickness, specimen width, HAZ size, and indentation. The other group of variables includes material properties, which are Young's modulus ( $E$ ), Poisson's ratio ( $\nu$ ), yield strength ( $\sigma_y$ ), ultimate tensile strength ( $\sigma_{uts}$ ), and elongation ( $e$ ). Since the material structures in nugget, HAZ, and base metal are different, different material properties are used for each part of the weldment. However, they are not independent material properties of the nugget and the HAZ can be approximately linked to those of the base

metal by hardness ( $H_v$ ) with the following relations (Ref. 14):

$$\sigma_{uts} = \sigma_0 + k_1 \cdot H_v \quad (6A)$$

$$\sigma_y = k_1 \cdot H_v \quad (6B)$$

$$e = k_2 / H_v \quad (6C)$$

$$H_v = k \cdot H_{vbase} \quad (6D)$$

where  $k_1$ ,  $k_2$ , and  $k$  are constants,  $\sigma_{uts}$  is ultimate tensile strength,  $\sigma_y$  is yield strength, and  $e$  is elongation.  $H_v$  and  $H_{vbase}$  are hardness of the concerned part and that of the base metal, respectively. By using these equations, five fewer material variables are needed. Furthermore, if only steel is considered, the Young's modulus and Poisson's ratio can be fixed as constants ( $E = 210$  GPa and  $\nu = 0.3$ ). Therefore, in the design, only the base metal properties and the hardness ratio ( $k$ ) between the nugget and base metal are left as material variables. Weld attributes considered are sheet thickness ( $t$ ), sheet width ( $w$ ), HAZ size ( $h$ ), and indentation ( $t_i$ ).

Therefore, Equation 5 can be simplified as

$$P_{max} = f_P(t, w, h, t_i; \sigma_y, \sigma_{uts}, e, k) \quad (7A)$$

$$U_{max} = f_U(t, w, h, t_i; \sigma_y, \sigma_{uts}, e, k) \quad (7B)$$

$$W_{max} = f_W(t, w, h, t_i; \sigma_y, \sigma_{uts}, e, k) \quad (7C)$$

Table 1 lists the ranges of each design variable, which are needed in the statistical design.

### Latin Hypercube Design

The Latin hypercube method was

found very useful in conducting computer experiments (Refs. 15, 16). A class of orthogonal Latin hypercubes that preserve orthogonality among columns is available for this purpose. Applying an orthogonal Latin hypercube design to a computer experiment benefits the data analysis in two ways. First, it retains the orthogonality of traditional experimental designs. The estimates of linear effects of all factors are uncorrelated not only with each other but also with the estimates of all quadratic effects and bilinear interactions. Second, it facilitates nonparametric fitting procedures, because one can select good space-filling designs within the class of orthogonal Latin hypercubes according to selection criteria.

Table 2 is an optimal Latin hypercube design for eight variables based on the maximum distance criterion. By using the maximum distance criterion, the design points are uniformly distributed in the design space, which eliminates the random effects and ensures that all the points are not too far nor too close to each other. In this design, there are 33 levels for each variable, ranging from  $-16$  to  $16$  in coded scale. Figure 2 shows the distributions of design variables projected onto a space of any two variables. As mentioned in the last section, each variable has a design range. All ranges are evenly divided and distributed to the corresponding levels, which are given in Table 3. The results (outputs) are also given in the table.

In order to effectively conduct the experiment, a generic finite element model was developed so that changes of geometrical variables (width, thickness, nugget size, HAZ size, indentation) and material

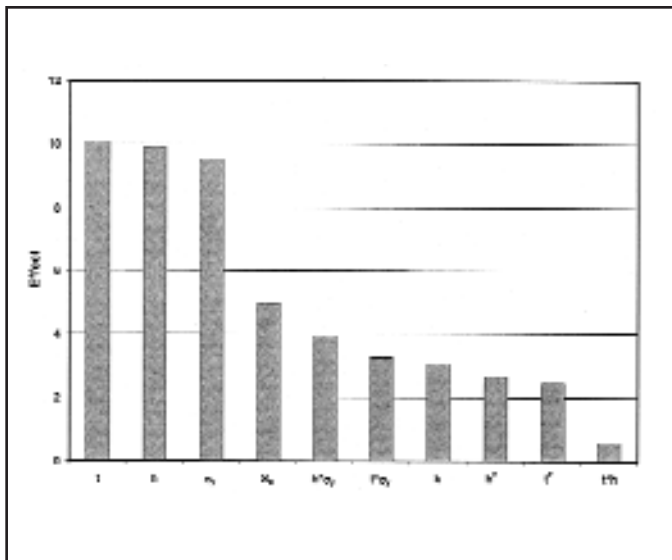


Fig. 5 — Variable effects on maximum energy  $W_{max}$ .

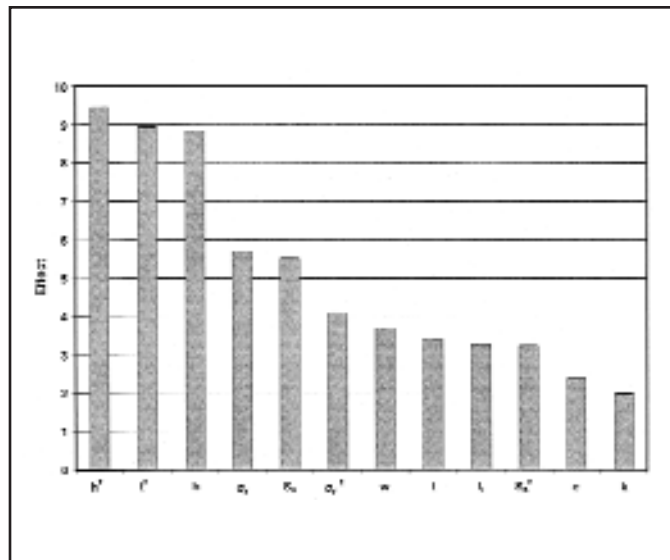


Fig. 6 — Variable effects on maximum displacement  $U_{max}$ .

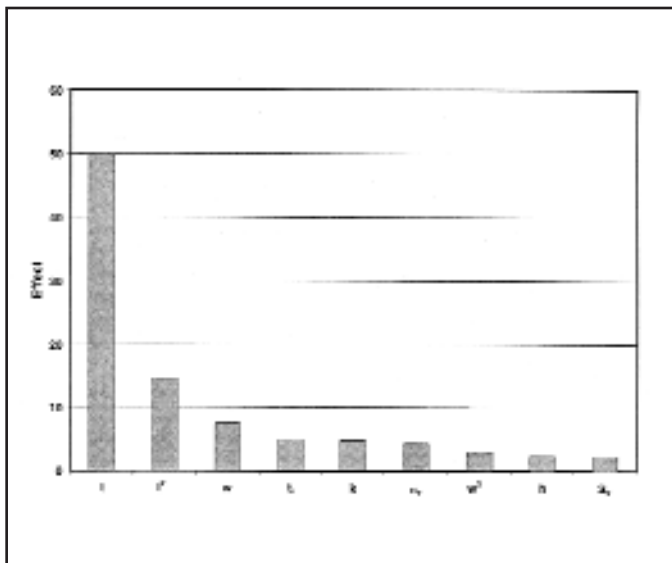


Fig. 7 — Variable effects on  $J^*$ .

## Results and Discussion

Using the results of Table 3, models of peak load, maximum displacement, and maximum energy can be derived by the regression method. Maximum load  $P_{max}$  is traditionally used to describe the quality of spot welds. Figure 4 shows the influences of variables on the maximum load  $P_{max}$ . It indicates yield strength and sheet thickness have the biggest influence of any of the variables. The size of the HAZ

ables,  $P_{max}$  can be expressed as

$$P_{max} = -6.74 + 2.72t + 0.016\sigma_y - 10.99h + 16.31t \cdot h \quad (9)$$

Statistically it still has a high coefficient of determination (94.5%). Regarding the confidence intervals of the coefficients, if 95% of confidence is considered, the intervals are [-15.86, 2.38], [-3.52, 8.97], [0.0128, 0.0197], [-19.90, -2.08], and [9.84, 22.79], respectively. Based on these intervals, the number of significant digits of the coefficients can be determined as shown in Equation 9. Although Equation 9 has a smaller coefficient of determination, it is preferred to Equation 8 for simplicity. As a matter of fact, it has a better “generality,” meaning it provides better predictions than Equation 8.

Following similar procedures, the expressions for  $W_{max}$  and  $U_{max}$  are obtained as shown in Equations 10 and 11. They have coefficients of determination of 97.6% and 97.0%, respectively.

$$W_{max} = 126966 - 414160t + 325520h - 106.718\sigma_y + 70.45\sigma_{uts} + 3288k - 6898.8t \cdot h + 22.50t \cdot \sigma_y + 26.916h \cdot \sigma_y + 164950t^2 - 204840h^2 \quad (10)$$

$$U_{max} = 3.41 - 12.49t + 10.26h - 0.012w - 1.07t_i - 0.0525\sigma_y + 0.0484\sigma_{uts} + 0.347e + 0.0644k + 5.05t^2 - 6.15h^2 + 0.00000226\sigma_y^2 - 0.000184(\sigma_{uts} - \sigma_y)^2 \quad (11)$$

variables (elastic and plastic properties in base metal, nugget, zones in the HAZ) can be easily implemented. A special code was developed for this purpose, which can automatically update the FEM model and design parameters.

The FEM model of a spot weld is shown in Fig. 3. There are 8021 nodes and 1452 C3D20R (20-node quadratic brick, reduce integration) elements using ABAQUS (Ref. 17). A fracture mechanics model is used to cope with the high-stress concentration existing around the nugget periphery. Different material properties are used for the nugget, heat-affected zones (HAZ), and the base metal.

also plays an important role in  $P_{max}$ . By selecting most of the effects,  $P_{max}$  can be expressed as

$$P_{max} = 2.64 - 32.18t + 32.08h - 59.70t_i - 0.0123\sigma_y + 0.0117\sigma_{uts} + 3.74k + 11.54t \cdot h + 0.0137t \cdot \sigma_y + 8.022h \cdot \sigma_y + t^2 - 0.00000372\sigma_y^2 + 0.00000936(\sigma_{uts} - \sigma_y)^2 + 224.94t_i^2 - 28.20h^2 \quad (8)$$

which has 99.3% of confidence of determination ( $R = 99.3\%$ ).

If only selecting sheet thickness  $t$ , yield strength  $\sigma_y$ , and size of HAZ  $h$  as vari-

able effects on maximum energy  $W_{max}$  and displacement  $U_{max}$  are shown in Figs. 5 and 6, respectively. Sheet thickness  $t$ , HAZ size  $h$ , and yield strength  $\sigma_y$  have the

greatest effects for  $W_{max}$ . But for maximum displacement, the most important variables are the quadratic terms of  $h$  and  $t$ , and linear term of  $h$ , and, therefore, the most important variable is the size of the HAZ. However, in both cases, some other terms, including quadratic and interactive terms, cannot be neglected in determining the maximum energy and displacement.

Beside maximum load  $P_{max}$ , maximum energy  $W_{max}$ , and displacement  $U_{max}$ , a fracture parameter J-integral (Ref. 18) was also evaluated, as it is an important parameter in the analysis of fracture mechanics. Using a normalized  $J^*$  as

$$J^* = \frac{J}{\frac{1}{E} \frac{F^2}{\pi d^3}} \quad (12)$$

where  $F$  is the applied load and  $d$  is the diameter of the nugget, the regression model of  $J^*$  can be expressed as

$$J^* = 2.14 - 5.41t - 0.0616h + 0.145w - 0.878t_1 - 0.0000998\sigma_y - 0.189e + 0.0854k + 1.70t^2 - 0.00198w^2 \quad (13)$$

It has a very high coefficient of determination of 99.6%. The effects of the variables considered are shown in Fig. 7.

The thickness has the dominant effect among all variables. Therefore, if only the thickness is chosen to express the J-integral, it will be

$$J^* = 3.34 - 1.61t + 0.656t^2 \quad (14)$$

The coefficient of determination is 97.4%, which means a fairly good approximation.

Based on these results, it is observed that the sheet thickness, HAZ size, and material yield strength are the most important attributes in determining a spot weld's strength or quality.

## Summary

In this investigation, attempts were made to link a weld's quality to its attributes under tensile-shear testing. The use of combined statistical design and analysis, and computer simulation provides a

systematic and effective means to deal with the multivariable nature of characterizing a spot weld. This study provides a basic understanding of the dependence of weld quality on both geometric variables and material properties. The findings can be summarized as follows:

- Effects of weld attributes, such as weld diameter, penetration, and indentation, can be analyzed through this integrated numerical analysis;

- The size of the HAZ plays an important role in the analysis of weld strength due to high stress concentration in and around the HAZ;

- Sheet thickness (and therefore nugget diameter), HAZ, and yield strength of base metal are the critical parameters in determination of spot welding quality.

- The present study also provides an estimate of J-integral, which may be used to describe the fracture behavior of a welded joint by treating the edge of a weld as a crack.

Although tensile-shear testing was used in the simulation, the method presented in this study can be extended to other loading modes such as cross-tension and fatigue.

## Acknowledgment

The authors are grateful for the financial support of Intelligent Resistance Welding Consortium, an Advanced Technology Program sponsored by NIST/DOC.

## References

1. American Welding Society, 2003. *Recommended Practice for Automotive Resistance Welding*. AWS D8.7 (Draft).
2. Spinella, D. J. 1994. Using fuzzy logic to determine operating parameters for resistance spot welding of aluminum. *Sheet Metal Welding Conference VI*, Detroit, Mich.
3. Newton, C. J., Browne, D. J., Thornton, M. C., Boomer, D. R., and Keay, B. F. 1994. The fundamentals of resistance spot welding aluminum. *Sheet Metal Welding Conference VI*, Detroit, Mich.
4. Keller, F., and Smith, D. W. 1944. Corre-

lation of the strength and structure of spot welds in aluminum alloys. *Welding Journal* 23(1): 23-s to 26-s.

5. McMaster, R. C., and Lindrall, F. C. 1946. The interpretation of radiographs of spot welds in alclad 24S-T and 75S-T aluminum alloys. *Welding Journal* 25(8): 707-s to 723-s.

6. Heuschkel, J. 1952. The expression of spot-weld properties. *Welding Journal* 31(10): 931-s to 943-s.

7. Sawhill, J. M., and Baker, J. C. 1980. Spot weldability of high-strength sheet steels. *Welding Journal* 59(1): 19-s to 30-s.

8. Thornton, P. M., Krause, A. R., and Davies, R. G. 1996. The aluminum spot weld. *Welding Journal* 75(3): 101-s to 108-s.

9. Ewing, K. W., Cheresch, M., Thompson, R., and Kukuchek, P. 1982. Static and impact strengths of spot-welded HSLA and low carbon steel joints. SAE Paper 820281.

10. Rivett, R. M. 1980. Factors affecting the quality of resistance spot welds. Ph.D. thesis, University of Wales.

11. Dickinson, D. 1981. Welding in the automotive industry. Committee of Sheet Steel Producers, Report 81-5, AISI.

12. Zuniga, S. M., and Sheppard, S. D. 1995. Determining the constitutive properties of the heat-affected zone in a resistance spot weld. *Modeling & Simulation in Materials Science & Engineering* 3(3): 391-416.

13. Gao, Z., and Zhang, K. 1997. Comparison of the fracture and fatigue properties of 16MnR steel weld metal, the HAZ and the base metal. *Journal of Materials Processing Technology* 63(1): 559-562.

14. Zhou, M., Zhang, H., and Hu, S. J. 1999. Critical specimen sizes for tensile shear tests. *Welding Journal* 78(9): 305-s to 313-s.

15. Koehler, J. R., and Owen, A. B. 1996. Computer experiments in *Design and Analysis of Experiments*. North-Holland, Amsterdam, pp. 261-308.

16. Ye, K. Q. 1998. Orthogonal column Latin hypercubes and their application in computer experiments. *Journal of the American Statistical Association* 93(444): 1430-1439.

17. *ABAQUS User's Manual* 5.8, Hibbit, Pawtucket, R.I.: Karlsson & Sorensen, Inc.

18. Rice, J. R. 1968. Mathematical analysis in the mechanics of fracture. *Fracture — An Advanced Treatise*. Vol. 2, M. Liebowitz, ed. New York, N.Y.: Academic, pp. 191-308.

## NOTICE

The paper "Numerical Simulation of Inertia Friction Welding Process by Finite Element Method," which was published in March 2003, pp. 65-s to 70-s, should have included the following acknowledgment:

The authors gratefully acknowledge the financial support by Bao-Steel Company of China. The authors also thank senior engineer Gao Dalu and Shi Weigin for their assistance in the experiments and Prof. Zhang Keshi and Prof. Li Shunping for their assistance in calculations.